GEOPHYSICS, VOL. 46, NO. 5 (MAY 1981); P. 781-795, 9 FIGS.

A self-similar model for sedimentary rocks with application to the dielectric constant of fused glass beads

P. N. Sen*, C. Scala*, and M. H. Cohen‡

ABSTRACT

We develop a theory for dielectric response of water-saturated rocks based on a realistic model of the pore space. The absence of a percolation threshold manifest in Archie's law, porecasts, electron-micrographs, and general theories of formation of detrital sedimentary rocks indicates that the pore spaces within such rocks remain interconnected to very low values of the porosity ϕ. In the simplest geometric model for which the conducting paths remain interconnected, each grain is envisioned to be coated with water. The dielectric constant of the assembly of water-coated grains is obtained by a self-consistent effective medium theory. In the dc limit, this gives Maxwell's relation for conductivity σ of the rock $\sigma = 2\sigma_w\phi/(3 - \phi)$, where σ_w is the conductivity of water. In order to include the local environmental effects around a grain, a self-similar model is generated by envisioning that each rock grain itself is coated with a skin made of other coated spheres; the coating at each level consists of other coated spheres. The self-consistent complex dielectric constant ε^* is given in this model in terms of that of water ε_w^* and of rock ε_m^*, by $[(\varepsilon_m^* - \varepsilon^*)/(\varepsilon_m^* - \varepsilon_w^*)][\varepsilon_w^*/\varepsilon^*]^{1/3} = \phi$ for spherical particles. This gives, in the dc limit, $\sigma = \sigma_w\phi^{3/2}$. For nonspherical particles, the exponent m in Archie's law $\sigma = \sigma_w\phi^m$ is greater than 3/2 for the plate-like grains or cylinders with axis perpendicular to the external field and smaller than 3/2 for plates or cylindrical particles with axis parallel to the external field. Artificial rocks with a wide range of porosities were made from glass beads. We present data on the glass bead rocks for dc conductivity and the dielectric constant at 1.1 GHz. The data follow the conductivity and the dielectric responses given by the self-similar model. The present theory fails to explain the salinity dependence of ε^* at lower frequencies.

INTRODUCTION

We study here the dielectric and conducting properties of water-saturated rocks. The real and imaginary parts of the dielectric constant ε' and ε'' and the dc conductivity σ appear in Maxwell's equations only as a combination, in the form of an effective dielectric constant $\varepsilon^*(\omega) = \varepsilon'(\omega) + i[\varepsilon''(\omega) + \sigma/\varepsilon_0\omega]$. Here ω is the circular frequency and ε_0 is the permittivity of free space. The real and imaginary parts of ε^* are related by the Kramers-Kronig relationship (Landau and Lifshitz, 1960). We compute ε^* as a function of frequency from the dc to GHz range based on a simple realistic model of pore space, i.e., the same geometric model and theory is used to predict both the dc conductivity σ and the high-frequency dielectric constant $\varepsilon'(\omega)$ of the rock.

In the next section, we review the shortcomings of the existing models and theories, leading to a realistic model for pore geometry. In general (see Ziman, 1979), the macroscopic properties of a composite material, containing phases with very different physical properties, depend not only on the volume fractions of the constituents, but are extremely sensitive to the geometry and topology of the boundary surfaces between the phases. The parameters of typical boundary surfaces in a mixture are not related in any simple way to the lowest order, point distribution functions for the constituents, so that the mathematical problem of calculating the overall properties of the system is very ill-posed (Ziman, 1979).

Nevertheless, many rocks show some "mean" behavior. For example, most of the rocks obey Archie's law [equation (1) below] which relates mean conductivity to the mean porosity alone (with some vague information about cementation contained in the exponent). This mean behavior has prompted us to seek out some mean universal features in the rock such that its properties can be explored analytically in some detail. In the section "Dielectric response in a self-similar model," we develop the theory of the complex dielectric response of a rock based on a simple, realistic geometric model that guarantees the continuity of the water-filled pore space. We show that the exponent m in equation (1) depends upon grain shape.

In order to understand dielectric properties of rocks better, we have done experiments with fused glass beads. The beads provide a clean system in which porosity, grain size, etc., can be controlled. In the section "Experimental results on fused glass beads and rocks," we present the measurements made in our laboratory at the dc and 1.1 GHz. The agreement between theory developed with our data and the high-frequency data of Poley et al (1978) (for frequencies $f > 0.5$ GHz) is remarkably good. A limited amount of data available on anisotropic grain agrees well with the shape-dependence of m prediction here.

In many rocks, the real part of the dielectric constant increases

Manuscript received by the Editor November 20, 1979; revised manuscript received August 20, 1980.
*Schlumberger-Doll Research, P.O. Box 307, Ridgefield, CT 06877.
‡James Franck Institute, University of Chicago, Chicago, IL 60637.

by several orders of magnitude as the frequency is lowered from the high megahertz range toward the dc value (see for example, Poley, 1978, and Keller, 1971). The magnitude of ε' increases generally with salinity of water. In the Discussion, we point out deficiencies of the simple model presented here and a few possible mechanisms that may explain the salinity, and also frequency dependences and high values of ε'.

REVIEW OF CURRENT DATA AND MODELS

We review the conductivity and dielectric data and theories behind them. We also review some geologic features of the pore space. We review briefly the very general theories of conduction in inhomogeneous media known as percolation theories. On the basis of these theories and other (geologic and electron micrographic) evidence, we conclude that the pore space in sedimentary rocks remains interconnected to very low values of porosity ϕ.

Many models, like complex refractive index (CRI) and Hanai-Bruggeman formulas (see below) that are used to predict high-frequency (megahertz to gigahertz range) dielectric constants, are shown to be inadequate. For example, in Hanai-Bruggeman formula for $\phi < 0.5$, there will be no dc conductivity since the derivation assumes that the water phase is in the form of isolated spheres embedded in a nonconducting rock host. Clearly, a correct geometrical model must be the basis of calculating both σ and $\varepsilon'(\omega)$ and should work at both high and low frequencies.

Using the measured values of dc electrical conductivity of a large number of brine-saturated cores, taken from a wide variety of sand formations, Archie (1942) found an empirical law

$$\sigma/\sigma_w = 1/F = a\,\phi^m. \tag{1}$$

Here σ_w is the water conductivity, F is the formation factor, ϕ the porosity, and m the cementation index. Archie took $a = 1$ in his original study. He found m varied between 1.8 and 2 for consolidated sandstones and found m to be 1.3 for unconsolidated sands packed in the laboratory. Since then, Archie's law has become an essential part of electric-log interpretation (Wyllie, 1963). Numerous other studies (see, for example, Wyllie and Gregory, 1953; Winsauer et al, 1952; Jackson et al, 1978, and references therein) have reconfirmed that equation (1) holds remarkably well for clay-free sedimentary rocks, with the value of a near 1 and values of m anywhere between 1.3 and 4, depending upon consolidation and other factors. Archie's law has been found to hold even for igneous rocks (Brace et al, 1968; Brace and Orange, 1968a, b).

The clays, capable of ion exchange, have complicated conduction mechanisms, and Archie's law does not hold for clayey rocks (Wyllie, 1963; Waxman and Smits, 1968). We shall not consider clayey or shaly rocks here.

There is no satisfactory theoretical explanation of the origin of Archie's law (Madden, 1976); the power law behavior, the nonzero conductivity to very low values of ϕ, and why the exponent in the power law is close to 2 are not understood. There are two main reasons: First, models such as a capillary tube model with little resemblance to real rock structures have been used in the past. The gross difference in pore structures in different rock types requires that different geometric models must be used for different classes. The second reason, which is closely related to the first, is that details of the rock geometry were not taken into account. Even in the formulation of empirical laws, the details of the geologic nature of the samples are generally ignored. Often, as we shall see below, the data could be represented better by laws, such as $\sigma = \sigma_w(\phi - \phi_c)^m$ with a nonzero ϕ_c, rather than as in equation (1).

In the following paragraphs we give a somewhat more elaborate description of specific models: (1) capillary tube models/network models, (2) percolation theories, and (3) effective medium theories for ε^*.

The capillary tube model (Wyllie and Rose, 1950; Schopper, 1966; Brace et al, 1968) does not give Archie's law from first principles. It is generally argued that the capillary tube length l with a sample of length L is given by $l = TL$, where T is tortuosity equal to $T = 1/\phi$ in order to reproduce Archie's law. The phenomenological relation between T and ϕ is not derived, but is chosen ad hoc to fit Archie's law. Furthermore, the branching nature of pore space is completely neglected. In a more sophisticated model of a network of interconnected tubes (Edmundson, 1978), the tube cross-sections were adjusted to reproduce equation (1). Greenberg and Brace (1969), Shankland and Waff (1974), and Madden (1976) also applied network models to sedimentary rocks. The branching nature in real pores in sedimentary rocks is far more complex than the simple network model assumed. Pore spaces in pore casts (Swanson, 1979) are connected, very

LIST OF SYMBOLS

a, b, c = Axes ellipsoids
Δv_k = Volume of rock grains added to the mixture at kth step.
ε^* = Complex dielectric constant = $\varepsilon' + i(\sigma/\omega\varepsilon_0 + \varepsilon'')$
ε' = Real part of the complex dielectric constant
ε'_m = Real part of the dielectric constant of the solid phase
ε''_w = Imaginary part of the water dielectric constant arising from rotation of water molecules alone
ε'' = Imaginary part of the dielectric constant without the conductivity terms $\sigma/\omega\varepsilon_0$
ε_0 = Permittivity of vacuum
ε_0^* = Complex dielectric constant of the assumed effective medium
ε_k^* = Complex dielectric constant at the kth step
ε_{k+1}^* = Complex dielectric constant at the $k + 1$th step
ε_w^* = Complex dielectric constant of water
ε_1^* = Complex dielectric constant of material 1
ε_2^* = Complex dielectric constant of material 2
ε_i^* = Complex dielectric constant of material i
f = Frequency
f_i = Volume fraction of the ith component
ϕ = Porosity
L = Depolarization factor
L_a = Depolarization factor along a-axis for a field impressed along a-axis
L_b = Depolarization factor along b-axis for a field impressed along b-axis
L_c = Depolarization factor along c-axis for a field impressed along c-axis
m = Exponent of ϕ in Archie's law
ω = $2\pi f$
σ = Conductivity
$\sigma(\omega)$ = The frequency dependence of conductivity shown explicitly
σ_w = dc conductivity of water
v = Volume of rock as a variable
V = Volume of water as a variable

irregularly and often look like irregularly connected thin sheets rather than tubes. It is hard to see the relevance of any network models, particularly those with a fixed coordination number. The interconnection of pore spaces is further evident from examination of electron micrographs. Although it is hard to draw conclusions about three-dimensional (3-D) connectivity from a two-dimensional (2-D) micrograph, a simple capillary model can be ruled out.

Quite general and powerful theories, collectively known as percolation theory, have been developed to describe the behavior of a random network of mixtures (Kirkpatrick, 1973). Since we shall draw upon the results of percolation theory, we mention a few salient points.

If the resistors (bonds) are removed randomly from a network, the conductivity of the network becomes zero when the fraction p_b of the remaining bonds falls below a critical value p_{cb}, known as the bond percolation threshold. If nodes, with all the resistors attached to the node, are removed randomly, the threshold is denoted by p_{cs}, the site percolation threshold. The value of p_{cj} ($j = s$ or b) depends upon the connectivity and dimensionality of lattice. For example, for a simple cubic array $p_{cb} = 0.25$, $p_{cs} = 0.31$. The conductance G of a random array is found to be (Kirkpatrick, 1973)

$$G = G_w(p_j - p_{cj})^{m_j}, \; j = s \text{ or } b. \tag{2}$$

Here G_w is the conductance of a bond. Kirkpatrick (1973) has found by numerical simulation that $m_j = 1.5$ for both bond and site problems near the critical region ($p_{cj} \leq p_j \leq p_{cj} + 0.2$), but $m_j = 1$ for greater values of p_j.

If the site percolation results are expressed in terms of fraction of bonds remaining, rather than number of sites remaining, G is found to be proportional to p_b^2. Shankland and Waff (1974) claim that $\sigma \propto \sigma_w\phi$ observed by Brace and Orange (1968a) in one set of experiments is explained by the bond percolation and $\sigma \propto \sigma_w\phi^2$, observed by Brace and Orange in another set of experiments (1968b) by site percolation. Furthermore, Shankland and Waff argue that $p_{cb} = 0$ because $p_{cb} \propto 1/t$ (Kirkpatrick, 1973), where t is the number of branches emanating from a site, and t tends to infinity.

The percolation theory of networks needs to be extended to the continuum case before it can be applied to the study of transport properties of inhomogeneous rocks. Since the continuum case can be generated either from the bond or from the site percolation problem, assigning of bond percolation in one case and site percolation in another case does not appear convincing.

Generalization of percolation theory to the continuum case was done by Webman et al (1976, 1977) and Straley (1978). The macroscopic conductivity shows scaling behavior

$$\sigma = a\,\sigma_w(\phi - \phi_c)^m, \quad \phi > \phi_c, \tag{3}$$

and

$$\sigma = 0 \qquad \phi < \phi_c. \tag{4}$$

The results of numerical simulation give $\phi_c = 0.145 \pm 0.005$ and $m = 1.4 \pm 0.05$, for ϕ close to ϕ_c. For $\phi > 0.4$, σ agrees well with the effective medium approximation result $\sigma = (3/2)\,\sigma_w(\phi - 1/3)$.

The value of ϕ_c in equation (4) depends upon the model of correlation chosen, and $\phi_c = 0.15$ is for a model with second-order bond correlation. For nearest neighbor correlation only, $\phi_c = 0.17$, and for the uncorrelated case, $\phi_c = 0.25$ (Webman et al, 1975). Thus the absence of a percolation threshold in Archie's law $\phi_c = 0$ implies that the fluid phase remains essentially continuous to very low values of the porosity, and the pore spaces in sedimentary rocks are strongly correlated.

Next consider the dielectric constant. In the literature, a large number of different formulas exist for the effective dielectric response ε^* of mixtures (Van Beek, 1967; Pascal, 1969) which are often used without ascertaining in each case whether the sample conforms to the geometry for which the formula holds. For example, the effective-medium theory (Webman et al, 1977) has a nonzero percolation threshold (33 percent) and should not be applied to data on rocks which do not show any finite percolation threshold.

For the 1.1-GHz electromagnetic propagation tool (EPT) of Schlumberger (Calvert et al, 1977), the so-called complex refractive index (CRI) formula has been used to interpret the results with some success (Freedman et al, 1979). The derivation assumes a model of parallel layers with layer thicknesses much greater than a wavelength, so the total transit time t for a pulse moving perpendicular to the layers is the sum of transit times t_i in each layer.

$$t = \sum_i t_i = \sum_i l_i \sqrt{\varepsilon_i^*}/c.$$

Here l_i is the thickness of each layer, ε_i^* is the complex dielectric constant of the ith layer, and c the velocity of light in free space. This immediately gives for the effective dielectric constant

$$\sqrt{\varepsilon^*} = \sum_i \phi_i \sqrt{\varepsilon_i^*},$$

where

$$\phi_i = l_i \Big/ \sum_i l_i$$

is the volume fraction of the ith phase. The rocks clearly do not have such a simple layered geometry in general. The typical distance l_i over which the dielectric constant varies is of the order of a pore or a grain size and is usually much smaller than the wavelength. Furthermore, a layer geometry gives zero dc conductivity, since current moving perpendicularly will be blocked by a rock layer.

Next, we review some geologic aspects of pore space. Sedimentary rocks are variable mixtures of precipitates and material worn or broken of other rocks. Nevertheless, sedimentary rocks are commonly and crudely divided into two broad classes, the detrital (also called clastic) and chemical. The former class arises from a mechanical deposition and is characterized by individual grains. The chemical rocks originate primarily from chemical precipitation and generally tend to be more homogeneous. Shales and sandstones are primarily detrital, while limestones are primarily chemical. These two types together account for over 95 percent of all sediments.

The interconnectedness of the pore spaces can be understood from examining the formation processes of the detrital sedimentary rocks. Two grains initially touch only at one point, leaving the intergranular space connected. Compression or depositing of a cementing mineral which reduces the pore space is self-limiting, and the pore space remains connected. For example, when pressure in the contact is high enough, the material moves out of the contact area. The pressure is reduced below that required for melting, and the process stops. The chemical deposition is also self-limiting —as the pore becomes smaller due to sedimentation, the flow decreases, and thereby sedimentation decreases. Although the models above are oversimplified, they help us understand how the percolation threshold could be zero.

The geometrical models for carbonate rocks are very different from those for detrital ones. For example, many samples of carbonate rocks show intragranular porosity and isolated pockets of pore spaces (Ham, 1962). The formation factor $F = \sigma_w/\sigma$ of such rocks would show a behavior $F \sim (\phi - \phi_c)^{-m}$, in contrast to Archie's law with $\phi_c = 0$. However, conduction data on rocks for which the pore spaces become disconnected below a percolation threshold are scarce.

Winsauer et al (1952) found that their data adhered to $\sigma = \sigma_w(\phi - 0.06)^{1.48}$, but abandoned this relationship and proposed what is known as the Humble formula: $\sigma = 1.61\ \sigma_w\phi^{2.15}$. By adjusting several parameters, Perez-Rosales (1976) casts Maxwell's formula [given by equation (15) below] $\sigma = \sigma_w 2\ \phi/(3 - \phi)$ into the form $\sigma = \sigma_w(\phi - \phi_c)/[M - (1 - M)\ \phi - \phi_c]$, and found ϕ_c varies from 0.02 to 0.1 and $M \approx 1.64$. For $M = 1.5$ and $\phi_c = 0$, his formula is identical to equation (15). However, the basis for the analysis of Perez-Rosales is not clear. In one case the low ϕ data of Wyllie and Gregory (1953), which show zero percolation threshold ($\phi_c = 0$) in the original form, are replotted to exhibit a nonzero ϕ_c. He also considered the data of Winsauer et al and found $\sigma = \sigma_w(\phi - \phi_c)/(1.75 - 0.85\ \phi)$. Although the value of ϕ used by Perez-Rosales agrees with Winsauer's value, this exponent of unity differs from 1.48 used by Winsauer et al for the same data.

Brace and Orange (1968b) found that rhyolite tuff (porosity of 40 percent) has much of its porosity in the form of round holes enclosed in volcanic glass. For this rock the conductivity is about a factor of ten less than that predicted by a simple Archie's law equation $\sigma = \sigma_w\phi^2$.

It is useful to measure formation factors of a suite of rocks in the laboratory to confirm the existence of a percolation threshold. Measurements on artificial rocks, mimicking carbonate rocks, will also be helpful. In general, it is easy to prepare samples exhibiting a percolation threshold (Abeles et al, 1975), but the requirement that the sample geometry correspond to that of real rocks must be imposed in these cases.

The discussion above illustrates the second difficulty we mentioned in understanding Archie's law: The empirical relations usually lump together data belonging to different classes of rocks. Archie (1942) noted that the exponent m in equation (1) varied with consolidation. There is much information contained in the prefactor a and the exponent m. This information is generally ignored even in empirical studies. Although partial lists (Keller and Frischknecht, 1966; Parkhomenko, 1967) relate (a, m) in equation (1) to a few geologic features of the rocks, more comprehensive studies should be undertaken.

In summary, Archie's law (1) holds empirically for a large range of detrital sedimentary rocks with the constant a near unity and with varying values of m. Theoretical treatments which purport to derive Archie's law pay inadequate attention to the geometry of the pore spaces, particularly to the implication that the pore space is connected.

DIELECTRIC RESPONSE IN A SELF-SIMILAR MODEL

We deliberately set out to make a model where the pore space is connected down to extremely low values of porosity, and we abandon tube models, network models, and percolation models.

Since we compute the dielectric constant in this model using the multiple scattering techniques currently in vogue in solid state physics, we digress here to recall a few salient results of these techniques.

It is often possible to divide physical behavior of a random system into two parts: an average property plus the fluctuations from it. In the solid state physics of a disordered system, the exact field is computed in terms of a multiple scattering theory in which fluctuations from the average medium are treated as perturbation. Thus, if we divide the rock into a large number of cells (for simplicity, we consider spherical cells here, although the result is generalized to other shapes in the Appendix) with a locally homogeneous dielectric constant ε_i^*, the electric field is computed as a sum of incident field propagating in an *assumed* homogeneous medium ε_0^* plus the fields scattered by fluctuations $\varepsilon_0^* - \varepsilon_i^*$. The multiple scattering formalism is exact. However, except for a few special cases, useful results are obtained only after making some approximation such as an approximation of statistical independence. This is known as single-site approximation. In this approximation, each particle or unit (an atom, or a locally homogeneous chunk of material) is subjected to a local field $\mathbf{E}^{(i)}$ which has been averaged over the configuration of all other particles, except the ith particle. Next, the macroscopic polarization is computed in terms of polarizability and the local fields. From the macroscopic polarization, one can compute the effective dielectric constant of the system (see Webman et al, 1977, for example).

$$\varepsilon^* = \varepsilon_0^*\left(1 + 2\sum_i f_i \frac{\varepsilon_i^* - \varepsilon_0^*}{\varepsilon_i^* + 2\varepsilon_0^*}\right)\left(1 - \sum_i f_i \frac{\varepsilon_i^* - \varepsilon_0^*}{\varepsilon_i^* + 2\varepsilon_0^*}\right)^{-1}. \tag{5}$$

In equation (5), f_i is the volume fraction of the ith phase.

Nonself-consistent calculation: $\varepsilon_0^* = \varepsilon_1$

For a two-component system, when a small concentration x of material ε_2^* is embedded as isolated spheres in ε_1^*, it is reasonable to choose $\varepsilon_0^* = \varepsilon_1^*$ in equation (5) to give

$$\frac{\varepsilon^* - \varepsilon_1^*}{\varepsilon^* + 2\varepsilon_1^*} = x\frac{\varepsilon_2^* - \varepsilon_1^*}{\varepsilon_2^* + 2\varepsilon_1^*}. \tag{6}$$

The approximation (6) has been derived in different contexts by Maxwell (1873, Dover ed., 1954), Maxwell-Garnett (1904), Wagner (1914), and Bottcher (1952) as a generalized Clausius-Mossotti-Lorentz-Lorenz relation. In solid state physics, equation (6) is known as the average t-matrix approximation (ATA).

Self-consistent calculation: $\varepsilon_0^* = \varepsilon^*$

We make a self-consistent approximation by setting $\varepsilon_0^* = \varepsilon^*$ in equation (5). The effective medium approximation of ε^* gives

$$\sum_i f_i\left[\frac{\varepsilon_i^* - \varepsilon^*}{\varepsilon_i^* + 2\varepsilon^*}\right] = 0. \tag{7}$$

Approximation (7) is known as the coherent potential approximation (CPA). Clearly, CPA treats all the components symmetrically, whereas ATA selects one as a host. It is not possible to describe here all the advantages of CPA over ATA without making technical remarks: The corrections to ε^* beyond CPA are fourth order in the transition matrix, whereas for ATA, the next order correction is second order in the scattering matrix. In practice, CPA has always agreed better with experiment than ATA (see discussions in Elliott et al, 1974; Ziman, 1979).

We now proceed directly to calculate the dielectric constant for our model. Summarizing the arguments given in the section, "Review of current data and models," the absence of a percolation threshold manifest in Archie's law, the electron micrographs, the pore casts, and the known sedimentation and diagenetic processes imply that the pore space remains connected in the first order of

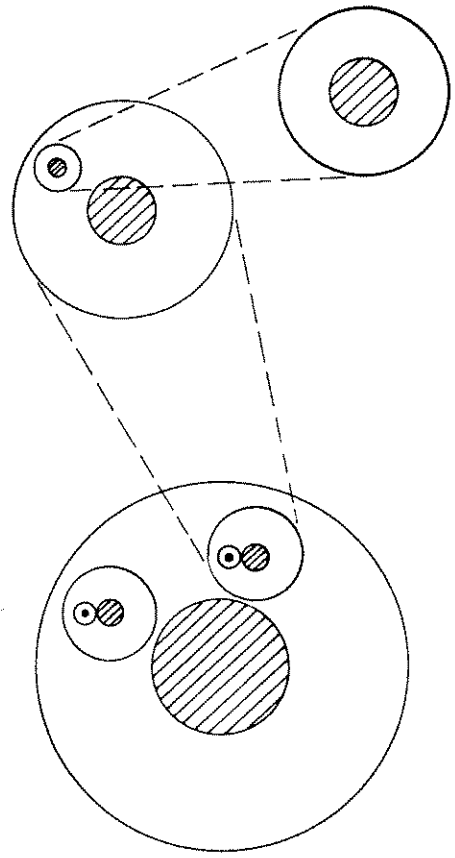

FIG. 1. Schematic diagram for the self-similar model of rock. Each unit in the rock is a grain coated with other coated spheres. The actual sizes are irrelevant and, therefore, all grain may have same or different sizes.

approximation, with the grains touching each other only at or on small, isolated regions of contact. Therefore, except at points which we approximate to be of measure zero, the grains are essentially coated with water. If we assemble the entire rock from rock grains of arbitrary size, coated with water, the continuity of the conduction path is guaranteed.

The polarizability α_i of a sphere i of dielectric constant ε_m^* uniformly coated with another material of dielectric constant ε_w^* has been calculated by Van de Hulst (1975, p. 74).

$$\alpha_i = b_i^3 \frac{(\varepsilon_w^* - 1)(\varepsilon_m^* + \varepsilon_w^*) + \eta_i(2\varepsilon_w^* + 1)(\varepsilon_m^* - \varepsilon_w^*)}{(\varepsilon_w^* + 2)(\varepsilon_m^* + \varepsilon_w^*) + \eta_i(\varepsilon_w^* - 1)(\varepsilon_m^* - \varepsilon_w^*)}. \quad (8)$$

Here b_i is the radius of the matrix sphere with its coating R_{mi} is the inner radius and $\eta_i = (R_{mi}/b_i)^3$ is the volume fraction of the inner sphere, and $\varepsilon_w^* = \varepsilon_w' + i\varepsilon_w'' + i\sigma_w/\omega\varepsilon_0$. Equation (8) implies that the coated sphere itself has a dielectric constant

$$\varepsilon_{CS}^{*(i)} = \frac{1 + 2\alpha_i/b_i^3}{1 - \alpha_i/b_i^3} = \varepsilon_w^* \left[\frac{\varepsilon_m^* + 2\varepsilon_w^* + 2\eta_i(\varepsilon_m^* - \varepsilon_w^*)}{\varepsilon_m^* + 2\varepsilon_w^* - \eta_i(\varepsilon_m^* - \varepsilon_w^*)} \right]. \quad (9)$$

The above results hold in the electroquasistatic limit $|k_i|b_i \ll 1$, where $k_i = \omega\sqrt{\varepsilon_i^*}/c$ is the wave vector of the field in the effective medium and in the components.

Using equation (7), the self-consistent dielectric constant of the rock made up of coated spheres is given by

$$\sum_i f_i \frac{\varepsilon^* - \varepsilon_{CS}^{*(i)}}{2\varepsilon^* + \varepsilon_{CS}^{*(i)}} = 0. \quad (10)$$

Here f_i is the volume fraction of the ith coated sphere in the assembly, i.e., volume of the ith sphere divided by the total volume of the rock. In general, f_i and η_i are unrelated.

The simplest case arises if we assume that $\eta_i = 1 - \phi$ is the same for all the spheres. Then, equations (10) and (11) give

$$\varepsilon^* = \varepsilon_w^* \left[\frac{\varepsilon_m^* + 2\varepsilon_w^* + 2(1 - \phi)(\varepsilon_m^* - \varepsilon_w^*)}{\varepsilon_m^* + 2\varepsilon_w^* - (1 - \phi)(\varepsilon_m^* - \varepsilon_w^*)} \right], \quad (11)$$

or

$$\frac{\varepsilon^* - \varepsilon_w^*}{\varepsilon^* + 2\varepsilon_w^*} = (1 - \phi) \frac{\varepsilon_m^* - \varepsilon_w^*}{\varepsilon_m^* + 2\varepsilon_w^*}. \quad (12)$$

Physically, equations (11) and (12) imply that the dielectric constant of the rock assembly is that of a coated sphere $\varepsilon^* = \varepsilon_{cs}^{*(i)}$. Thus, a coated sphere, embedded in the effective medium representing the rock, does not scatter the electromagnetic wave, since both have the same dielectric constants. Although equation (7) is the same in form as equation (12) for $\varepsilon_1^* = \varepsilon_w^*$, $\varepsilon_2^* = \varepsilon_m^*$ and $x = 1 - \phi$, the two equations are completely different in content. Equations (11) and (12) are derived as a self-consistent formula for coated spheres, and the question of which material is host and which one is impurity simply does not arise. In other words, for equations (11) and (12) the form is determined entirely by model geometry. To illustrate the difference, consider small ϕ. Taking water as the impurity, equation (6) gives

$$\varepsilon^* = \varepsilon_m^* \left[\frac{\varepsilon_w^* + 2\varepsilon_m^* + 2\phi(\varepsilon_w^* - \varepsilon_m^*)}{\varepsilon_w^* + 2\varepsilon_m^* - \phi(\varepsilon_w^* - \varepsilon_m^*)} \right], \quad (13)$$

which is similar to equation (11) with ε_m^* and ε_w^*, and ϕ and $(1 - \phi)$ interchanged. Assume that the matrix is nonconducting, and solving for Im ε^* with $\varepsilon_w'' = \varepsilon_m'' = 0$ in equation (13) gives

$$\sigma = \sigma_m[(1 + 2\phi)/(1 - \phi)], \quad (14)$$
$$= 0, \quad \text{for} \quad \sigma_m = 0.$$

On the other hand, equation (12) gives

$$\sigma = \sigma_w[2\phi/(3 - \phi)]. \quad (15)$$

Therefore, for $\phi < 0.5$, equation (6) or (14) implies that the rock would be insulating, whereas equation (12) or (15) finds it to be conducting.

Since equation (7) is only an ATA for uncoated spheres, but equation (12) is a CPA, the latter gives a far superior formula in this case where the geometry is explicitly taken into account. This has already been pointed out by Smith (1977). The analog of equation (12) for metallic spheres coated with ceramics, the so-called cermets, has been widely used.

Formula (15) gives $\sigma \propto \phi^m$ with $m = 1$ for small ϕ. The empirical evidence for an exponent m greater than unity is overwhelming, both from laboratory and field data. Accordingly, we must regard the model of a sphere coated with a spherical shell of water of fixed proportions as overly simple.

The single-site or mean-field approximation such as CPA fails to take into account variety of *local* environments of each type of rock grain. The systematic way around this problem is to consider bigger and bigger clusters, where a grain is not only surrounded by water but also surrounded by other rock grains. In practice this problem is extremely difficult numerically and has been solved only for a few special cases. We proceed here by a very simple intuitive method of incorporating the clustering

effects in a single-site effective medium theory. Assume that the spheres are coated with a skin made of coated spheres, the coating at each level consisting of other coated spheres. First assume that we add a few grains of rock of any size to water. (We emphasize again as long as the inequality $b_i\ \omega|\sqrt{\varepsilon_i^*}|/C \ll 1$ holds, the size of the particles is irrelevant.) Then use this mixture to coat some new grains, and so on. At each step we add a small amount of grain, and we determine the dielectric constant self-consistently. If ε_k^* is the dielectric constant of the mixture at a given step k and we use this to coat additional grains of a small total volume Δv_k, of rock, then using equation (12), we find the self-consistent dielectric constant ε_{k+1}^* of the mixture is given by

$$\frac{\varepsilon_{k+1}^* - \varepsilon_k^*}{\varepsilon_{k+1}^* + 2\varepsilon_k^*} = \frac{\Delta v_k}{V + v}\,\frac{\varepsilon_m^* - \varepsilon_k^*}{\varepsilon_m^* + 2\varepsilon_k^*}. \tag{16}$$

Here V and v are the total volume of water and rock, respectively, at that step. For an infinitesimal increment dv, equation (16) gives

$$\frac{d\varepsilon^*}{3\varepsilon^*} = \frac{dv}{V + v}\,\frac{\varepsilon_m^* - \varepsilon^*}{\varepsilon_m^* + 2\varepsilon^*}. \tag{17}$$

Here ε^* is the dielectric constant of the mixture that is used to coat the additional grains of (total) volume dv. The volume fraction of the rock matrix is given by

$$\Psi = \frac{v}{V + v}. \tag{18}$$

Differentiating equation (18) gives

$$d\Psi = (1 - \Psi)\,\frac{dv}{V + v}. \tag{19}$$

Using equation (19) in equation (17) gives

$$\frac{d\varepsilon^*}{3\varepsilon^*} = \frac{d\Psi}{1 - \Psi}\,\frac{\varepsilon_m^* - \varepsilon^*}{\varepsilon_m^* + 2\varepsilon^*}. \tag{20}$$

Integrating equation (20) from $\Psi = 0$ to $\Psi = 1 - \phi$ with the boundary condition that $\varepsilon^* = \varepsilon_w^*$ for $\Psi = 0$ gives

$$\left(\frac{\varepsilon_m^* - \varepsilon^*}{\varepsilon_m^* - \varepsilon_w^*}\right)\left(\frac{\varepsilon_w^*}{\varepsilon^*}\right)^{1/3} = \phi. \tag{21}$$

The dielectric constant of the effective medium ε^* is obtained by solving equation (21) for (given) ε_m^*, ε_w^*, and ϕ. Apart from taking the local environment effects more correctly, this method has another good feature. Each time, only an infinitesimal amount of perturbation is added to the parent material. The self-consistent approximation CPA (used here at each step) gives a very good result when the concentration of perturbation tends to zero (Ziman 1979; Elliott et al, 1974). Secondly, the geometrical model has a self-similarity often seen in rocks, i.e., the rock appears to be the same at any magnification. The geometrical configuration at the final stage is schematically shown in Figure 1. This geometry bears a close resemblance to the multiple scale picture of networks employed by Madden (1976).

Equation (21) is identical to the Hanai-Bruggeman formula in form, but it is quite different in content. Hanai (1968) and Bruggeman (1935) start with the nonself-consistent result [equation (6)] and allow the impurity concentration to grow. For $\phi < 0.5$, for example, they start with rock as host, and with infinitesimal amount of water embedded, as *isolated* spheres, in it. In the next stage, they add more water, as isolated spheres, and use the previous mixture as a host, and so on, using equation (6) at each stage. Although this has an advantage of introducing an infinitesimal perturbation at each stage, it produces (at each stage) a non-conducting rock. In other words, Hanai-Bruggeman gives the dielectric constant in terms of the dielectric constants of the host and of the impurity and the impurity concentration. For $\phi < 0.5$, Hanai-Bruggeman gives, instead of equation (21), a formula like equation (21) with ε_m^* and ε_w^* interchanged and ϕ replaced by $1 - \phi$, and hence a zero dc conductivity. Our formula (21) bears a similar relation to the Hanai-Bruggeman as the CPA formula (15) bears to the ATA formula (14). In the present case, the form of equation (21) is fixed by the geometry, and no confusion arises between host and impurity.

The limiting cases of equation (21) are quite instructive. As the frequency ω tends to zero, $\varepsilon^* = \varepsilon' + i\varepsilon'' + i\,\sigma/\omega\varepsilon_0$ tends to infinity as $i\,\sigma/\omega\varepsilon_0$. Separating the imaginary part, when $\varepsilon'' = 0$, one finds

$$\sigma = \sigma_w \phi^{3/2}. \tag{22}$$

The dc limit given by equation (22) holds for frequencies for which inequalities $\sigma_w \gg \varepsilon_0\omega(\varepsilon_w' - \varepsilon_m')$ and $\sigma \gg \varepsilon_0\omega(\varepsilon' - \varepsilon_m')$ hold. In this limit, keeping up to first-order terms in $(\varepsilon_w' - \varepsilon_m')/\varepsilon_0\omega\sigma_w$ and separating imaginary parts gives equation (22), and the real part gives

$$\varepsilon' = \frac{3}{2}\,\varepsilon_m' + \phi^{3/2}\left(\varepsilon_w' - \frac{3}{2}\,\varepsilon_m'\right). \tag{23}$$

This result obtains the correct limit of $\varepsilon' = \varepsilon_w'$, for $\phi = 1$, but disagrees at very small ϕ, where the inequality $\sigma \gg \omega\varepsilon_0(\varepsilon' - \varepsilon_m')$ no longer holds. According to equation (22), $\sigma = \sigma_w\phi^{3/2}$ goes to zero as ϕ goes to zero. From equation (21), we find directly that $\varepsilon' = \varepsilon_m'$, $\sigma = 0$ for $\phi = 0$.

Equation (23) shows an Archie type behavior. Since ε_m' and ε_w' are usually known, equation (23) can be used to obtain the water-filled porosity without knowing the water conductivity σ_w. It is usually difficult to measure σ_w in a borehole.

In the Appendix, we show that the exponent can be different from 3/2 for different shapes. Madden also finds $m = 1.5$ for the $\omega = 0$ case by an argument similar to that of Hanai-Bruggeman (Madden, 1978).

In the high-frequency limit ($\omega \to \infty$), assuming ε_m' and ε_w' independent of frequency, equation (21) gives

$$\left(\frac{\varepsilon' - \varepsilon_m'}{\varepsilon_w' - \varepsilon_m'}\right)\left(\frac{\varepsilon_w'}{\varepsilon'}\right)^{1/3} = \phi, \tag{24}$$

and

$$\sigma = \sigma_w\,\frac{(2\varepsilon_w' + \varepsilon_m')\varepsilon'(\varepsilon' - \varepsilon_m')}{(2\varepsilon_w' + \varepsilon_m')\varepsilon_w'(\varepsilon_w' - \varepsilon_m')}. \tag{25}$$

For the case where $\varepsilon_m' \ll \varepsilon_w'$, ε', equations (24) and (25) combine to give

$$\varepsilon' = \phi^{3/2}\varepsilon_w', \tag{26}$$

and

$$\sigma = \phi^{3/2}\sigma_w. \tag{27}$$

Thus for the practical cases where $\varepsilon_m' \ll \varepsilon_w'$ (ε_m' and ε_w' are frequency independent), a comparison between dc result given by equations (22) and (23) and the high-frequency results given by equations (26) and (27) implies that the variation of ε' and σ with frequency is not great (see Figure 9). In the next section, we show that there is experimental evidence to the contrary.

In the next section, the results obtained here are applied to measurements we have made on fused glass beads and to data in the literature.

EXPERIMENTAL RESULTS ON FUSED GLASS BEADS AND ROCKS

We now compare with theory the dielectric constant on artificial rocks made of fused glass beads at 1.1 GHz and conductivity at 120 Hz that we measure in our laboratory. As will be seen, the agreement with theory developed in the last section is excellent. We also compare our theory with published data, and point out difficulties and limitations of the present theory. Under certain circumstances (for low salinities and for high frequency at high salinity), the agreement between experimental data in literature and theory is also excellent.

Sample preparation

Glass beads in the size range of 210 and 250 μm were obtained from Analabs, North Haven, Connecticut. For the work reported here, bead size was restricted to this single cut, but measurements on unfused beads at 1.1 GHz were made on sizes from 297 to 88 μm. No influence of size over this range was noted.

The artificial rocks were prepared by fusion at 710°C in 20-cm long carbon or Atomergic Chemetals vitreous carbon molds in a Lindburg crucible furnace under nitrogen atmosphere. The lower porosities were obtained by lengthening the fusion time at 710°C. This was followed by a carefully controlled annealing and cooling schedule to prevent stress cracking. No cracks were observed on SEM or optical examination. Rod lengths were trimmed to size, with a diamond saw, using methanol as a coolant, carefully redried at 110°C, and stored over silica gel.

Sample porosities and the grain and bulk densities were determined by a buoyancy technique, following vacuum impregnation with the desired solution.

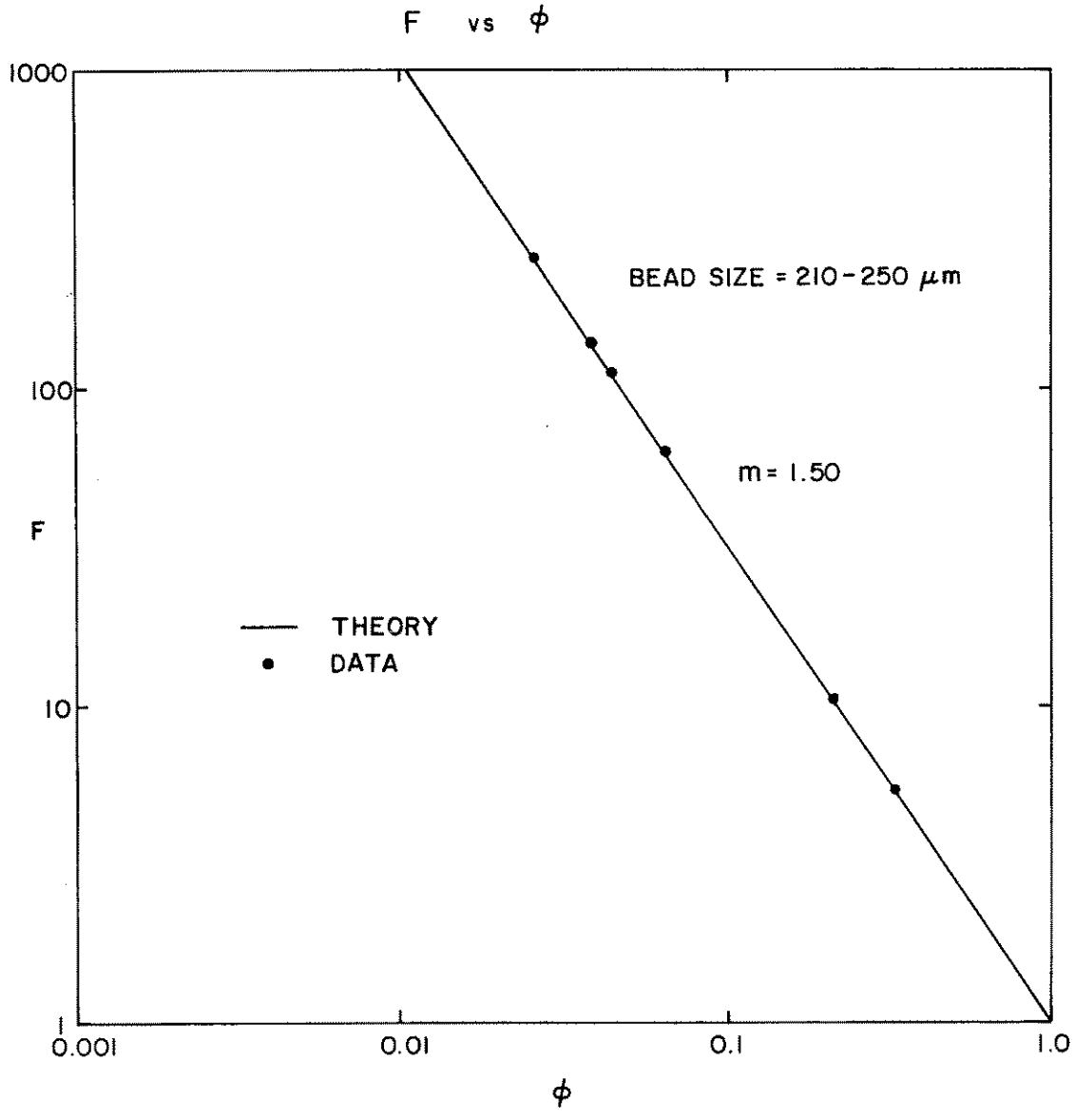

FIG. 2. Conductivity of fused glass beads as a function of porosity showing $\sigma = \sigma_w \phi^{3/2}$ behavior. The size of grains in the self-similar model can all be the same (as here) or all different. Hanai-Bruggeman formula would give $\sigma = 0$ for $\phi < 0.5$.

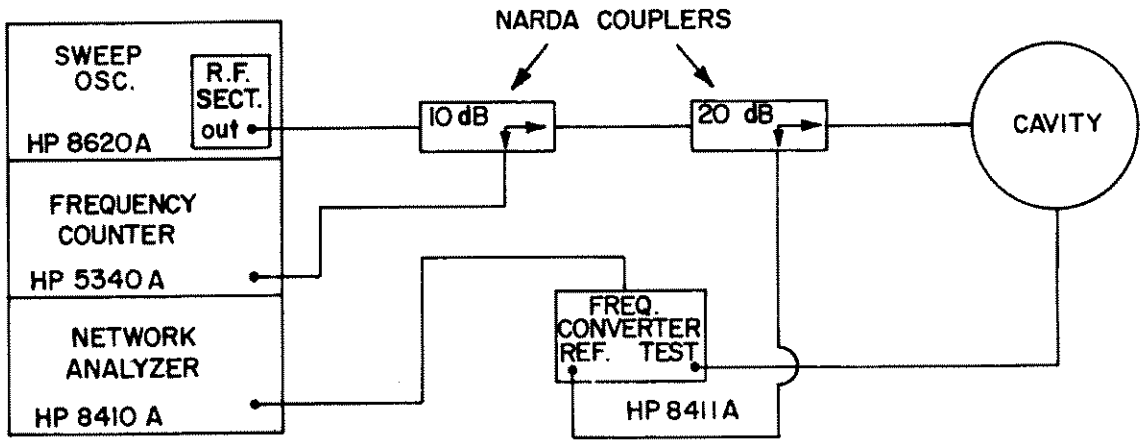

FIG. 3. Block diagram of cavity system used to measure dielectric response at 1.1 GHz.

Low-frequency conductivity

Low-frequency (120 Hz) in-phase conductivity measurements with artificial rocks saturated in 10.1, 1.0, and 0.10 Ω-m NaCl solutions were made in a two-electrode cell with a Hewlett-Packard 4261A LCR meter. Spring tensioned silver electrodes contacted the sample through soft porous silver Selas filtration membranes (0.45 μm pore size). Capacitance was too low to measure. Internal salinities were changed by diffusion at 85°C for more than 16 hours in baths with volumes at least 10^3 larger than the pore volume. This process was repeated until the desired invariant solution resistivity was attained.

The agreement between the theoretical low-frequency result given by equation (22) and the experimental results shown in Figure 2 is excellent. The values of porosity go as low as 2 percent, and we do not find any percolation threshold.

High-frequency ε*

1.1 GHz measurements were made in a TM(010) cavity system

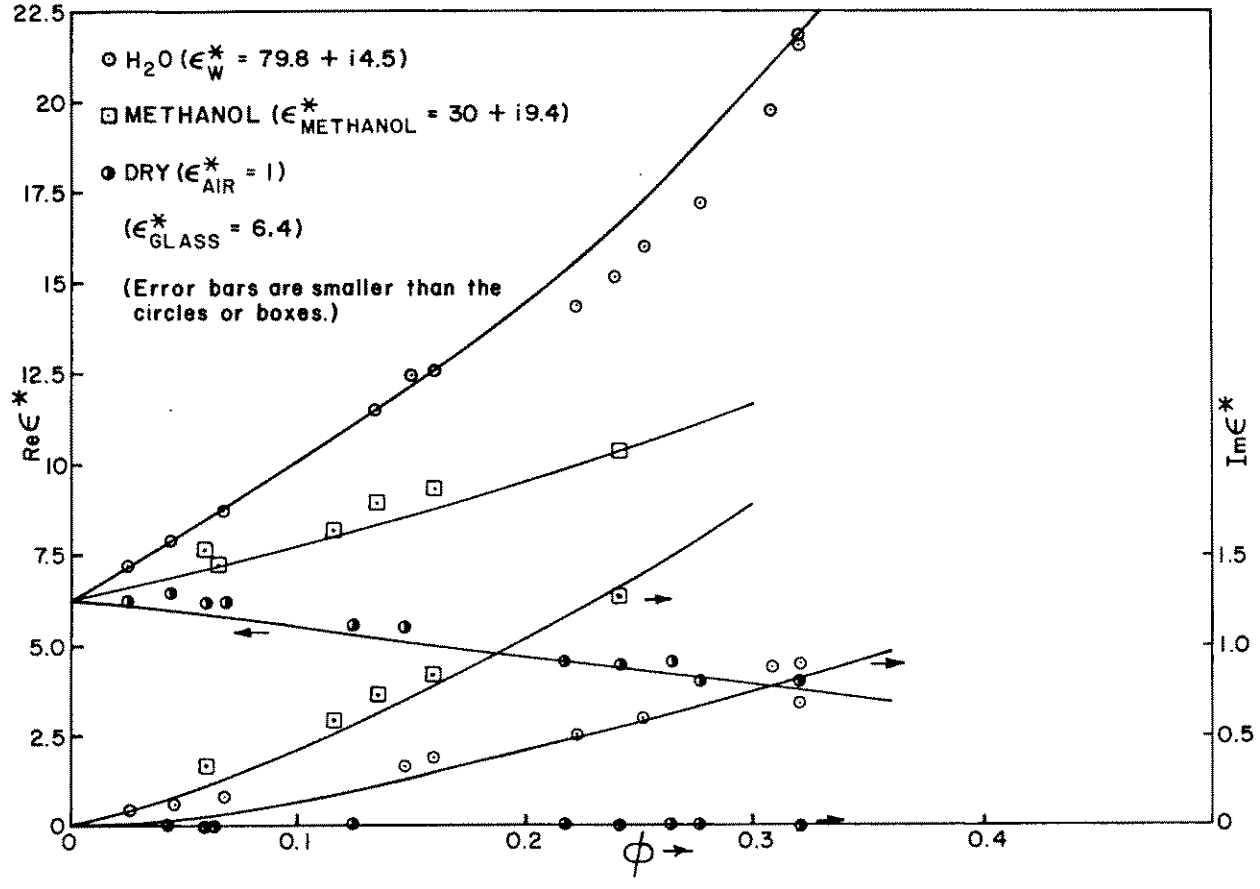

FIG. 4. Real part ε′ and imaginary part $\varepsilon'' + \sigma/\omega\varepsilon_0$ of the dielectric constant ε* for fused glass beads at 1.1 GHz as a function of porosity and saturated with distilled water, methanol, and air, respectively (measured by us). The lines are theoretical predictions. The dielectric constant of pure water and methanol at 1.1 GHz are (79.8 + *i*4.5) and (30 + *i*9.4), respectively. The value of ε'_m for glass is 6.4.

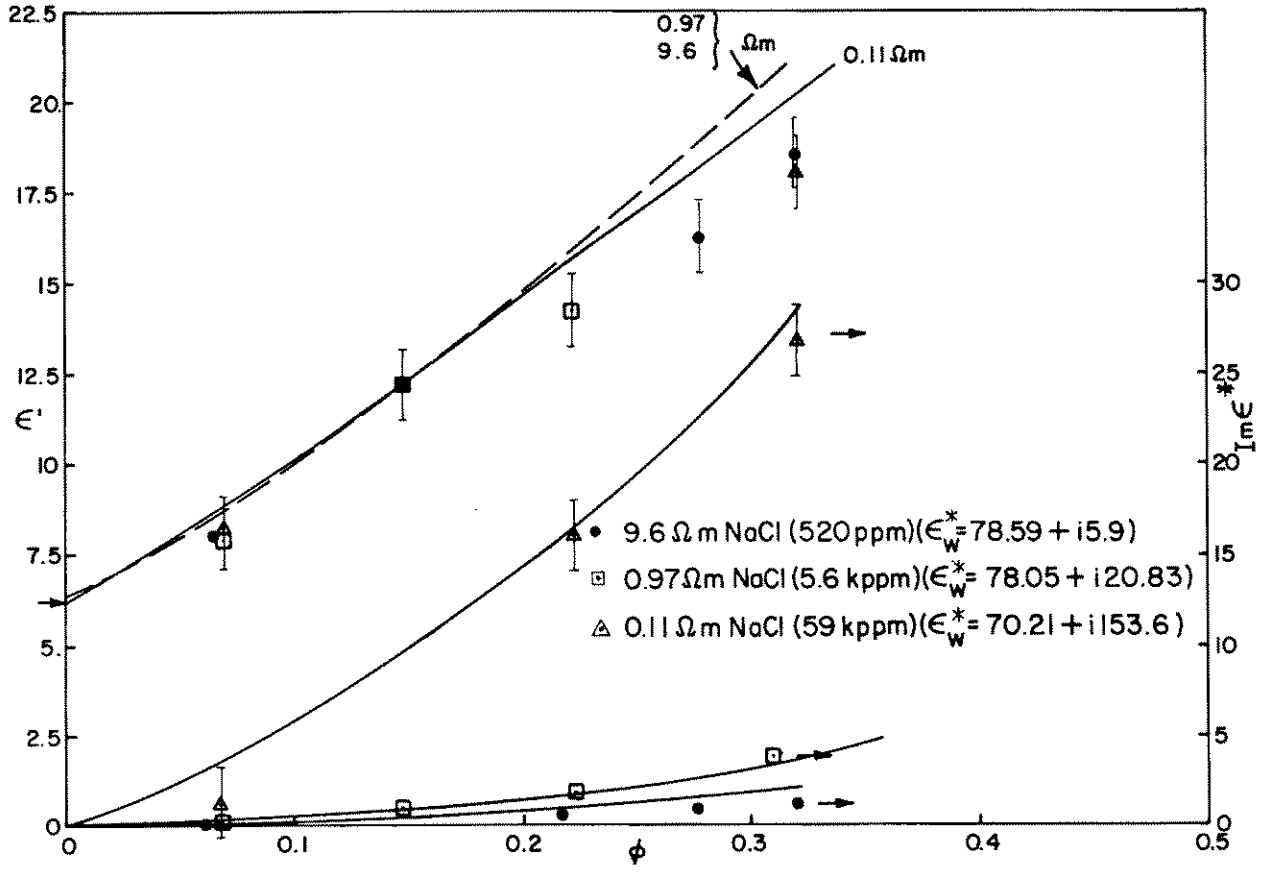

FIG. 5. Imaginary part $\varepsilon'' + \sigma/\omega\varepsilon_0$ and real part ε' of the dielectric constant ε^* for fused glass beads at 1.1 GHz as a function of porosity, saturated with saline water (measured by us). The lines are theoretical predictions. The dielectric constants of water at various NaCl concentrations are $(70.21 + i153.6)$ for 0.11 Ω-m, $(78.05 + i20.83)$ for 0.97 Ω-m, and $(78.59 + i5.9)$ for 9.6 Ω-m solutions. The real part of ε' computed from our model is practically indistinguishable between 9.6 and 0.97 Ω-m solution.

(Rau and Bizer, 1976). The block diagram is shown in Figure 3. A sample of known volume is introduced into the high Q resonant cavity, and dielectric constants ε' and $\varepsilon'' + \sigma/\omega\varepsilon_0$ are measured by determining the shift in cavity frequency and decrease in quality factor. System accuracy was checked with pure liquids of known dielectric. Accuracy of Re ε^* and Im ε^* with samples with $Q > 100$ is better than 1 percent. Samples with lower Q, $50 < Q < 100$, have estimated accuracies of 10 percent. Measured values of Re ε^* and Im ε^* for the samples filled with air, distilled water, and methanol have an accuracy of 1 percent and those filled with NaCl, 10 percent.

For the measurement at 1.1 GHz and a bead size 0.01 cm, $|k| < 0.1\ \text{cm}^{-1}$, so $|k|b \ll 1$ holds. The real part ε' and imaginary parts $\varepsilon'' + \sigma/\omega\varepsilon_0$ of the dielectric constant ε^* are plotted against porosity in Figure 4 for distilled water and methanol. The agreement of theory with experiment is excellent. The imaginary part $\varepsilon'' + \sigma/\omega\varepsilon_0$ and real part ε' as functions of porosity are shown in Figure 5 for saline water. The agreement is again good. For dry glass beads, ε'' remains zero. However, for wet glass beads, ε'' extrapolates to a very small but nonzero value as a function of porosity at zero porosity; it may be due to interfacial phenomena taking place in the interface of glass and solution. For example, salinization of the glass surface by water could cause an increase in surface conductance and ion concentration. A test with cyclohexane, a less polar, ionizable liquid than water, gave lower ε'' values. These additional surface mechanisms lie outside the scope of the present investigation and have to be treated separately (see the next section).

Application to real rocks

Next we consider application to data of the theory available in literature. Equation (22) is one of the well-known forms of Archie's law. Archie found for clean unconsolidated sandstones $\sigma = \sigma_w\phi^m$, $m = 1.3$, which is not far from 1.5 as predicted above. Wyllie and Gregory (1953) found that adherence to $\sigma = \sigma_w\phi^{1.3}$ was good for spherical glass beads with $0.25 > \phi > 0.10$, and that σ decreases for shapes different from spheres.

Jackson et al (1978) did systematic experiments with uncompacted sands, both natural and artificial. They found that adherence to Archie's law $\sigma = \sigma_w\phi^m$ is good, and that the exponent m depends upon the shape of the particle, increasing as the particles become less spherical, varying from about 1.2 for spheres to 1.9 for platey shell fragments. They find little dependence of m on the size or size distribution. For a suite of 8 marine sands (with sphericity 0.8), they find $m \approx 1.5$, varying from 1.4 to 1.58. For artificial glass beads (spheres), they find $m \approx 1.2$; for rounded sand commercial sand (sphericity 1.83), $m \approx 1.4$; and shaley sand (sphericity 0.78) $m \approx 1.52$; and for shell fragments (sphericity 0.5), $m \approx 1.85$. These observations are in qualitative agreement with the results obtained in the Appendix where we show $m > 3/2$

for platey materials. For the case when σ_m is nonzero, the dc form of equation (21) gives $[(\sigma_m - \sigma)/(\sigma_m - \sigma_w)]\,(\sigma_w/\sigma)^{1/3} = \phi$, which a number of experimentalists, including Hanai (1968), Pearce et al (1973), and Wobschall (1977), found to agree with experiments quite well.

There are a large number of experimental data on ε^* of rocks. Often such details as porosity and salinity of the water are missing, and a direct comparison is ruled out. For present purposes, we consider the data obtained by Poley et al (1978). Their results may be incorrect, because of the electrode polarization effects at lower frequencies, but at high frequencies the electrode polarization effects are small. For illustration, we compare data from their Figures 13a and 13b for sandstones, Figure 16b for calcite, and Figure 18 for sandstones. If the values of Im $\varepsilon^* = \varepsilon'' + \sigma/\omega\varepsilon_0$ are much greater than Re ε^*, then the limiting equations (22) and (23) hold. As a matter of fact, these limiting forms hold even if Im ε^* fails to be much greater than Re ε^*, as noted below equations (26) and (27). In other words, since equation (21) shows little frequency dependence, we can use its low-frequency value over a wide frequency range for all practical purposes (Figure 9). At 1.2 GHz, we have to include the dielectric loss ε''_w of water, and the complete form of equation (22) becomes

$$\text{Im } \varepsilon^* = (\sigma_w/\omega\varepsilon_0 + \varepsilon''_w)\phi^{3.2}. \tag{28}$$

Note that Poley et al (1978) wrote $\varepsilon^* = \varepsilon' + i\varepsilon''$, and therefore they included the conduction losses in their ε''. In Figures 6 and 7, dashed lines represent equation (28). The agreement is good at low values of salinity but poor at higher values of salinity. Similar agreement is obtained for data given in Figures 16c, 13b, 13c, and Figure 14 of Poley et al (1978).

In Figure 8 we reproduce as plotted points the values of ε' at 500 MHz observed by Poley et al, along with a curve representing

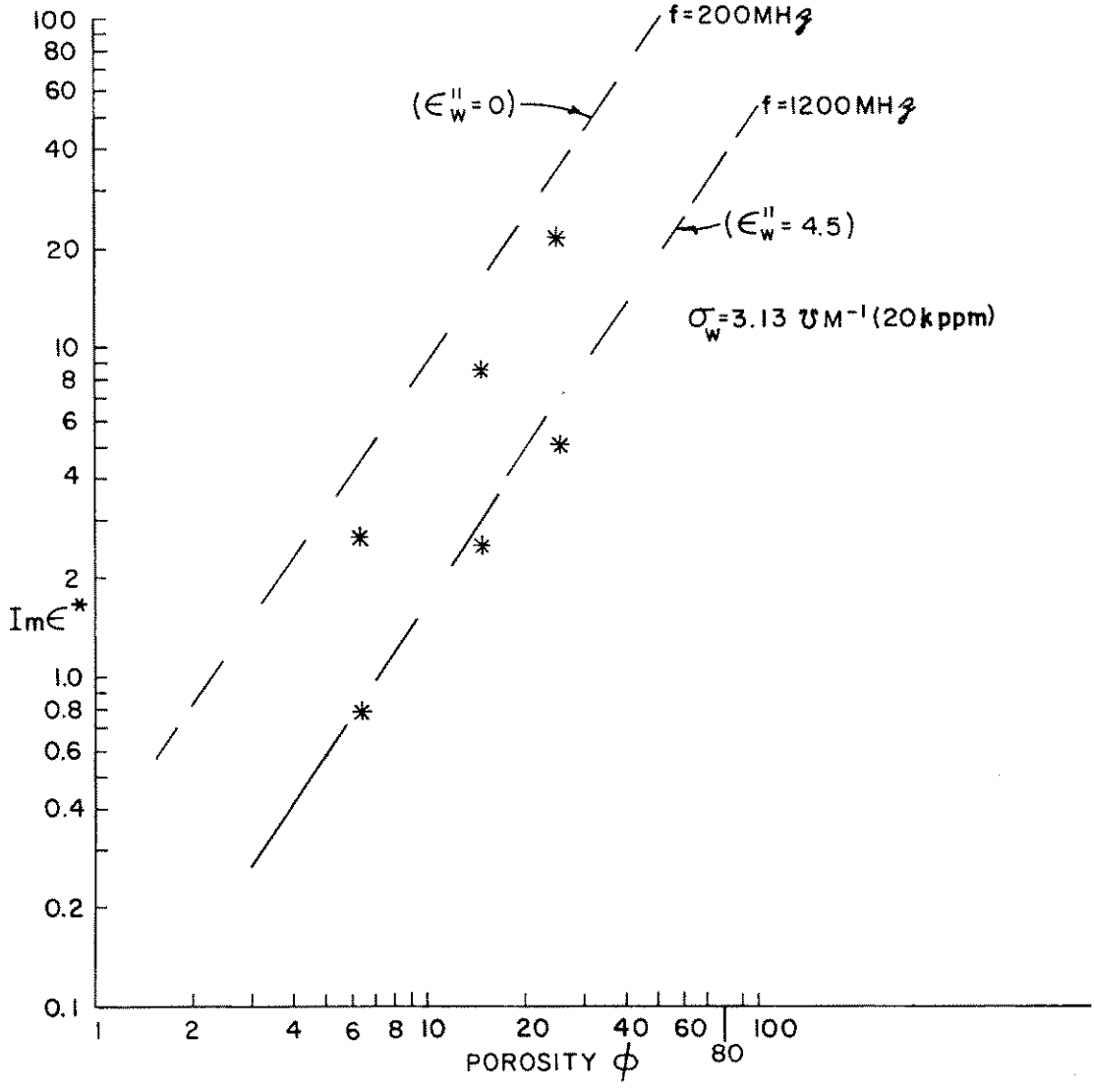

FIG. 6. Variation of the Im $\varepsilon^* = \sigma/\omega\varepsilon_0 + \varepsilon''$ as a function of porosity and salinity. The experimental points are from Poley et al (1978), at f = 200 and 1200 MHz for sandstones. The dashed lines are theoretical ones given by equation (28). Hanai-Bruggeman formula gives Im $\varepsilon^* = 0$ for $\phi < 0.5$.

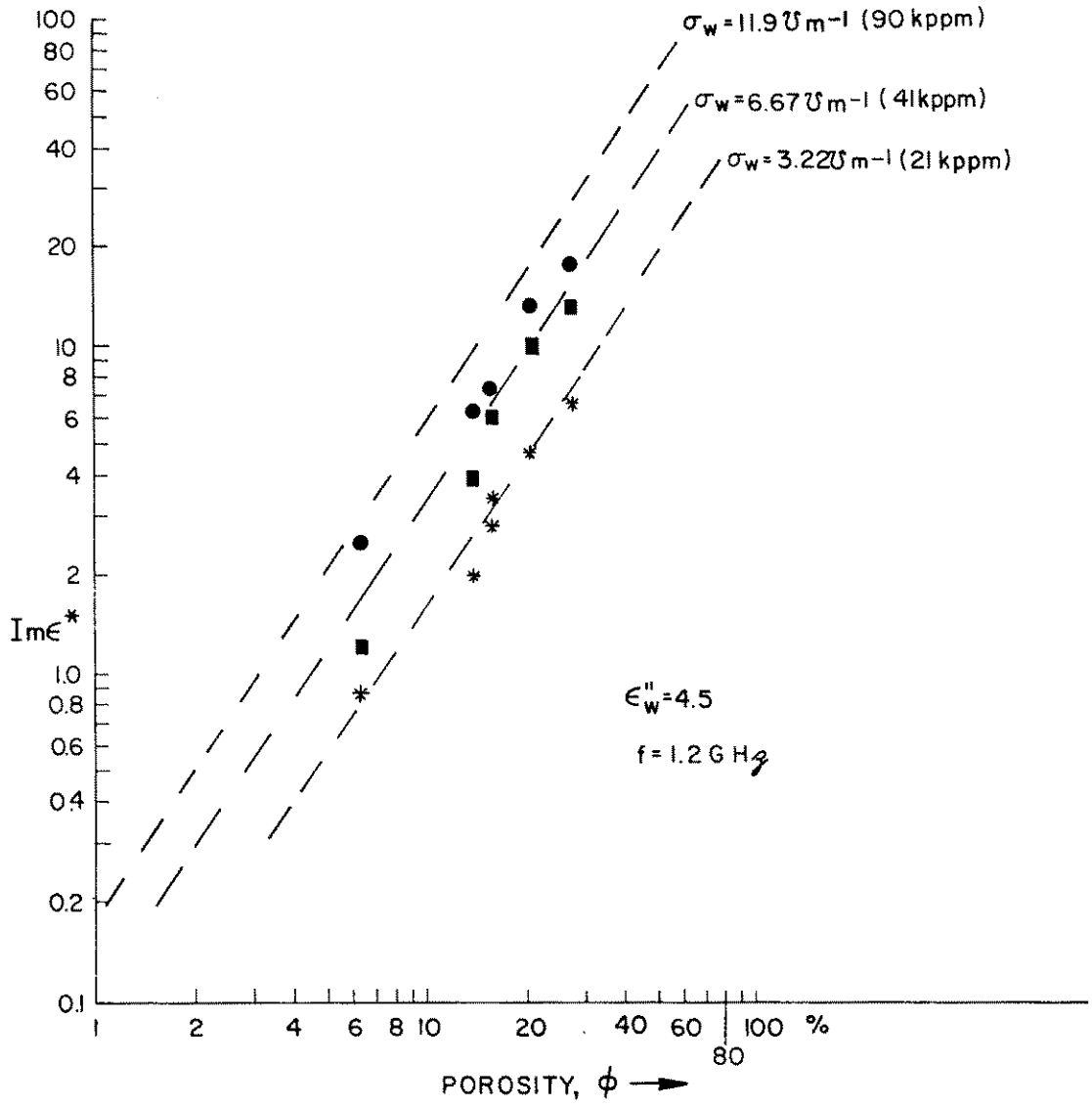

FIG. 7. Variation of Im $\varepsilon^* = \sigma/\omega\varepsilon_0 + \varepsilon''$ as a function of porosity for limestones at three different salinities. The dashed lines are theoretical result [equation (28)]. Hanai-Bruggeman formula gives Im $\varepsilon^* = 0$ for $\phi < 0.5$.

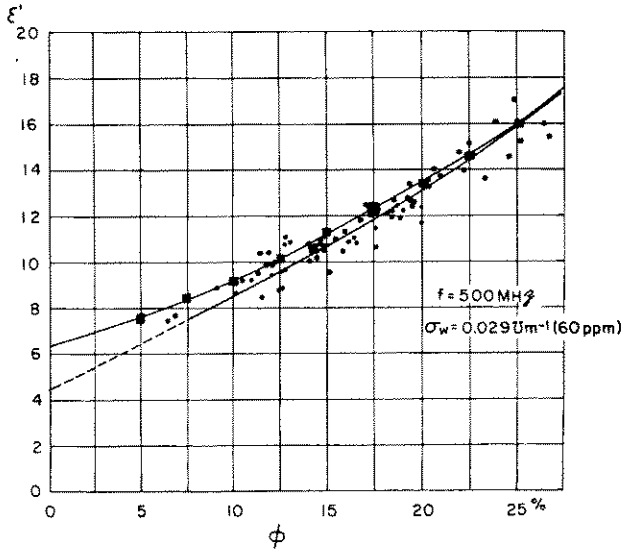

FIG. 8. Variation of real part of the dielectric constant ε' at 500 MHz of fresh water-saturated clean sandstones (dots and the lower line) plotted as function of porosity from Figure 18 of Poley et al (1978). Boxes denote theoretical prediction made by self-similar model. ($\sigma_w = 0.029\ \Omega\text{-m}^{-1}$ estimated from Figure 3 of Poley et al.) The boxes are connected by a line.

the theoretical results obtained from the self-similar model [equation (21)] using $\varepsilon'_m = 4.6$ (quartz value) and $\varepsilon'_w = 80, \sigma_w = 0.029$ Ω^{-1}-m^{-1} estimated from Figure 3 of Poley, for fresh water.

The excellent agreement with theory and experiment may be somewhat misleading, since the agreement at lower frequencies (and at higher salinities) is rather poor (see the next section).

DISCUSSION

The model described here is a first step in treating the geometry of interconnected pore space correctly. Several important aspects of the pore geometry have been neglected, and there are experimental results that show the need to treat these aspects more carefully. We will briefly discuss these aspects here.

As mentioned in the Introduction, the macroscopic properties of the rock depend upon the detailed geometry and topology of the boundary surface between the rock and water. A theory like the one developed here which involves average porosity alone cannot be sufficiently correct. For example, in Figure 4 of Poley et al (1978), we find that ε' for two samples with porosities of 12.7 and 12.9 percent, respectively, are drastically different, yet the ε' at about 10 MHz for two samples with porosities as far apart as 12.9 and 24.6 percent is the same.

Next, consider the variation of ε^* over a large-frequency range. We showed by the low-frequency limit given by equation (24) and the high-frequency limit given by (26) that ε' did not vary much over the frequency range. In Figure 9 we plotted ε' and σ computed by equation (21) for fused glass beads. The value of ε' does not show much change over the great frequency range we have used here. (The high-frequency result in Figure 9 is for illustrative purposes, so we have neglected ε''_w for clarity, due to water around 1 GHz, for this plot *only*.) At frequency near 10^8 Hz, theoretical results show a resonance effect. This can be understood by rewriting equation (7) as a Debye type formula. For spheres of glass dispersed in water, the resonance frequency from equation (6) is given by

$$f = \frac{1.8 \times 10^{10}(3 - \phi)\sigma_w}{2\varepsilon'_w + \varepsilon'_m + (1 - \phi)(\varepsilon'_w - \varepsilon'_m)}.$$

Thus for fused glass beads of porosity $\phi = 0.09$, $\sigma_w = 4.55$ Ω^{-1}-m^{-1} and $\varepsilon'_w \approx 80$, $\varepsilon'_m = 4.67$, this gives $f = 1.2 \times 10^9$ Hz. The vestiges of this persist somewhat even in self-similar models. Note that f varies as σ_w, but the changes in ε' observed by Poley et al (1978) are much too large to be explained by the values predicted by the self-similar model.

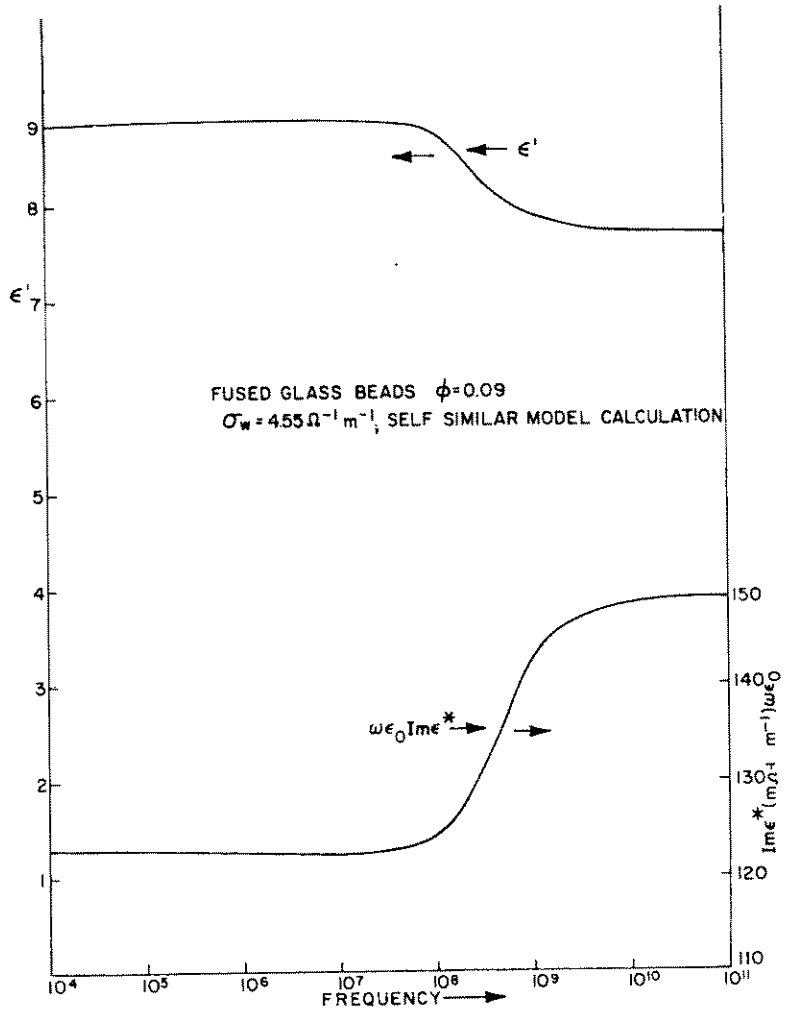

FIG. 9. Variation of ε', Im ε^* as a function of $f = \omega/2\pi$. The lines are obtained by using equation (21).

There are two obvious aspects that we have neglected here that contribute to these high values of ε'. One is some detailed aspect of geometry (textural), and the other is electrochemical effects at the rock-water interface. We briefly discuss these below.

First, consider textural features. The effect of grain contact was neglected. The patches of surfaces where the grains touch will not contribute to depolarization. Thus, we have overestimated the depolarization effects. The effect of touching is similar to, and in some cases is a consequence of, the effect of different shapes. Shape effects are discussed in the Appendix.

In the model, all the pore spaces were assumed to be interconnected. Thus the effects of dead-end pore spaces are not accounted for properly. A dead-end pore space is somewhat isolated from the main conducting paths, like a dangling branch connected only by one of its two ends to a network. Since electric current is blocked by the wall of the dead end, no current can flow. This can be modeled by a local field in a connected branch, canceling the macroscopic field. Such local fields may give rise to the large dielectric constant, since the effect of dielectric constant is to reduce the applied field.

The dead ends will not contribute to the conductivity, but can give rise to a high value of ε' at low frequency. As a crude model for the dead end, we assume that a few isolated spheres of water coated with quartz are embedded in the rock. A preliminary estimate shows that the magnitude of the rise in ε' in this model could explain the measured data. The detailed results will be published elsewhere. The difference in number of dead ends may be responsible for differences in $\varepsilon'(\omega)$ for two samples of similar porosity, as mentioned above.

Next consider the interfacial electrochemical double layer at the rock-water interface. This has a big effect on SP, induced polarization, and resistivity measurements (Keller, 1971). The clays show particularly high surface activity, and small amounts of clay can change $\varepsilon'(\omega)$ drastically from that predicted by equation (21) at low frequencies. Hoyer and Rumble (1976) found a correlation between clay content and dielectric constant in the 10 Hz–1 kHz range.

As long as the criterion $|k|b \ll 1$ is met, i.e., the wavelength of the radiation is much greater than a typical distance over which ε' and σ fluctuate in the material, it can be shown that the dielectric response of the inhomogeneous medium is scale invariant (Cohen, 1979). Thus, without interface effects, at long wavelengths the dielectric measurements cannot be used to estimate size. Meador and Cox (1975) claimed that they found an exponent-c (for $c = 1/2$, the complex refractive index formula is obtained) that depends upon size. Although their formula is ad hoc, an empirical relation between size and dielectric constant would imply surface effects.

It is interesting to note that the effective medium approximation predicts that real part of dielectric constant $\mathrm{Re}\,\varepsilon^* \propto 1/\sqrt{\omega}$, near percolation threshold. Although it may be tempting to use this result to explain high values of dielectric constants at low values of frequency ω, it would be wrong to apply this result for values of porosity significantly greater than zero, since the percolation threshold for rocks appears to be zero.

Next consider the case when the water saturation is not 100 percent and hydrocarbons are present. For water-wet rocks, we expect that the analysis given in the text applies with (slight) modification of ε_m^* to a mixture of ε_m^* and hydrocarbons. In this case, oil blobs can be treated essentially in the same manner as the water-coated rock grains were treated, and we expect no percolation threshold as $\omega \to 0$, $\sigma = \sigma_w(S_w\phi)^m$, where S_w denotes the volume fraction of the pore space occupied by conducting water. In the oil-wet rocks, on the other hand, below a critical value S_{wc} the water phase will be broken up into unconnected regimes, and we expect a nonzero percolation threshold S_{wc}: $\lim_{\omega \to 0} \sigma = \sigma_w(S_w\phi - S_{wc}\phi)^m$. This is a highly interesting three-phase mixture problem, where the percolation threshold depends upon the concentration of one of the phases itself. We are currently investigating this situation.

ACKNOWLEDGMENTS

We are indebted to P. Lacour-Gayet, W. Kenyon, Prof. T. Madden, E. Hunt, and R. P. Porter for useful discussions. We would also like to thank A. Capiello and M. Ridge for help with the experiments. We would like to thank B. Fuller, F. Segesman, W. Kenyon, and the editorial staff and the reviewers of GEOPHYSICS for their critical remarks on the manuscript.

Postscript.—After this manuscript was finished, K. Mendelsson pointed out that an equation similar to equation (21) was obtained for *magnetic* systems by A. K. Veinberg (1967, Soviet Phys. Doklady, v. 11, p. 593) by yet another method. Veinberg does *not* consider coated spheres. He considers self-consistent effective medium theory. His treatment amounts to computing ε_k^* of a mixture of rock and water, then adding an infinitesimal amount of rock and recomputing ε_{k+1}^* using a fraction of the previous mixture and the newly added rock as two components, and so on, step by step. Since an effective medium theory in general shows a percolation threshold at a given stage, it is not clear why the Veinberg model does not predict a percolation threshold in the final step, if one starts from the rock end and builds up water concentration step by step. However, we expect the water phase to remain interconnected if we start to displace water step by step. This may not be a serious difficulty, since in actual geologic processes in general the rock phase gradually builds up by displacing the water phase. It is also interesting to note that at low concentration, Clausius-Mossotti or ATA gives the same result as the effective medium theory or CPA (see Elliott et al, 1974). Therefore, Veinberg's approach of adding infinitesimal amounts of grain in steps and applying effective medium theory at each step yields the same result as the Hanai-Bruggeman approach. The latter approach consists of adding infinitesimal amount of grain but applying Clausius-Mossotti theory at each step.

REFERENCES

Abeles, B., Pinch, H. L., and Gittelman, J. I., 1975, Percolation conductivity in granular WAl_2O_3 metal film: Phys. Rev. Lett., v. 35, p. 247–252.

Archie, G. E., 1942, The electrical resistivity log as an aid in determining some reservoir characteristics: Trans. AIME, v. 146, p. 54–62.

Bottcher, C. J. F., 1952, Theory of electric polarization: 1st ed., Elsevier, Amsterdam, sec. 64, p. 415.

Brace, W. F., and Orange, A. S., 1968a, Electrical resistivity changes in saturated rocks during fracture and frictional sliding: J. Geophys. Res., v. 73, p. 1433–1445.

———— 1968b, Further studies of the effects of pressure on electrical resistivity of rocks: J. Geophys. Res., v. 73, p. 5407–5420.

Brace, W. F., Walsh, J. B., and Frangos, W. T., 1968, Permeability of granite under high pressure: J. Geophys. Res., v. 73, p. 2225–2236.

Bruggeman, D. A. G., 1935, Berechnung Verschiedener Physikalischer Konstanten von Hetarogenen Substanzen: Ann. Phys. Lpz., v. 24, p. 636–679.

Calvert, T. J., Rau, R. N., and Wells, L. E., 1974, Electromagnetic propagation, a new dimension in logging: SPE paper no. 6542.

Cohen, M. H., 1979, Scale invariance of low-frequency electrical properties: Unpublished.

Edmundson, H., 1978, Unpublished report: Schlumberger-Doll Research Center.

Elliott, R. J., Krumhansl, J. A., and Leath, P. L., 1974, The theory and properties of randomly disordered crystals and related physical systems: Rev. Mod. Phys. v. 46, p. 465.

Freedman, R., and Vogiatzis, J. P., 1979, Theory of microwave dielectric

constant logging, using the electromagnetic propagation method: Geophysics, v. 44, p. 969–986.
Fricke, H., 1924, A mathematical treatment of the electric conductivity and capacity of disperse systems: Phys. Rev., v. 24, p. 575–587.
Greenberg, R. J., and Brace, W. F., 1969, Archie's law for rocks modelled by simple networks of resistors: J. Geophys. Rev., v. 74, p. 2099–2102.
Ham, W. E., Ed., 1962, Classification of carbonate rocks: AAPG, Tulsa.
Hanai, T., 1968, Electrical properties of emulsions, *in* Emulsion science: P. Sherman, Ed., New York, Academic Press.
Hoyer, W. A., and Rumble, R. C., 1976, Dielectric constant of rocks as a petrophysical parameter: SPWLA 17th Annual Logging Symp. June 1–12.
Jackson, P. D., Taylor-Smith, D. and Stanford, P. N., 1978, Resistivity-porosity-particle shape relationships for marine sands: Geophysics, v. 43, p. 1250–1262.
Keller, G. V., 1971, Electrical characteristics of the earth's crust, *in* Electromagnetic probing in geophysics: J. R. Wait, Ed., Boulder, Golem Press.
Keller, G. V., and Frishknecht, F. C., 1966, Electrical methods in geophysical prospecting: Oxford, Pergamon Press, p. 517.
Kirkpatrick, S., 1973, Percolation and conduction: Rev. Mod. Phys., v. 45, p. 574–588.
Landau, L. D., and Lifshitz, E., 1960, Electrodynamics of continuous media: New York, Pergamon Press.
Madden, T. R., 1976, Random network and mixing laws: Geophysics, v. 41, p. 1104–1124.
——— 1978, Effects of porosity and fluids on physical properties of rocks: Unpublished.
Maxwell, J. C., 1954, A treatise on electricity and magnetism: (1873), New York, Dover Publications, Inc.
Maxwell-Garnett, J. C., 1904, Trans. Roy. Soc., London, v. 203, p. 385.
Meador, R. A., and Cox, P. T., 1975, Dielectric constant logging, a salinity independent estimation of formation water volume: SPE paper 5504.
Mendelson, K. S., and Cohen, M. H., 1979, The effect of grain anisotropy on the electrical properties of isotropic sedimentary rocks: Unpublished.
Parkhomenko, E. I., 1967, Electrical properties of rocks: New York, Plenum, p. 314.
Pascal, H., 1964, On the dielectric constant of the saturated porous medium and the possibility of its application to the geophysical investigation of oil wells: Rev. Roum. Sci. Tech. Mech. Appl., v. 9, p. 601.
Pearce, D. C., Hulse, W. H., Jr., and Walker, J. W., 1973, The application of the theory of heterogeneous dielectrics to low surface area soil systems: IEEE trans. Geosci. Electr., v. GI-11, p. 167–170.
Perez-Rosales, C., 1976, Generalization of the Maxwell equation for formation resistivity factors: J. Petr. Tech., v. 38, p. 819.
Poley, J. Ph., Nooteboom, J. J., and de Waal, P. J., 1978, Use of VHF dielectric measurement for borehole formations analysis: Log Analyst, p. 8–30.
Rau, R. N., and Bizer, H., 1976, Dielectric measurements of water-saturated cores using resonant cavity method: Private communication.
Schopper, J. R., 1966, A theoretical investigation on the formation factor/permeability/porosity relationship using a network model: Geophys. Prosp., v. 14, p. 301–341.
Shankland, R. J., and Waff, H. S., 1974, Conductivity in fluid-bearing rock: J. Geophys. Res., v. 79, p. 4863–4871.
Smith, G. B., 1977, Dielectric constants for mixed media: J. Phys. D., v. 10, p. L39–L42.
Sprunt, E. S., and Nur, A., 1977, Resolution of porosity through pressure solution: Geophysics, v. 42, p. 726–738.
Straley, J. P., 1978, Critical phenomena in resistor networks: J. Phys., v. C9, p. 783–795.
Stratton, J. A., 1941, Electromagnetic theory: New York, McGraw-Hill Book Co., Inc.
Swanson, B. F., 1979, Visualizing pores and nonwetting phase in porous rock: J. Pet. Tech. v. 31, p. 10–18.
Van Beek, L. K. H., 1967, Dielectric behavior of heterogeneous systems, *in* Progress in dielectrics: J. P. Birks, Ed., London, v. 7, Iliffe Books Ltd.
Van de Hulst, H. C., 1957, Light-scattering by small particles: New York, Wiley and Sons.
Wagner, K. W., 1914, Erklarung der Dielektrischen Nachwirkungen auf Grund Maxwellscher Vortellungen: Arch. Electr., v. 2, p. 371–387.
Waxman, M. H., and Smits, L. J. M., 1968, Electrical conductivities in oil-bearing shaly sands: SPE J., p. 107–122; paper 1863A SPE 42nd Annual Fall Meeting, Houston, Oct. 1–4, 1967.
Webman, I., Jortner, J., and Cohen, M. H., 1967, Numerical simulation of continuous percolation conductivity: Phys. Rev., v. B14, p. 4737–4740.
——— 1975, Numerical simulation of electrical conductivity in microscopically inhomogeneous materials: Phys. Rev., v. B11, p. 2885–2892.
——— 1977, Theory of optical and microwave properties of microscopically inhomogeneous materials: Phys. Rev., v. B15, p. 5712–5723.
Winsauer, W. O., Shearin, H. M., Masson, P. H., and Williams, M., 1952, Resistivity of brine-saturated sands in relation to pore geometry: AAPG Bull., v. 36, p. 253–277.
Wobschall, D., 1977, A theory of complex dielectric permittivity of soil containing water: Semidisperse model: IEEE Trans. Geosci. Electr., v. G1–18, p. 49–58.
Wyllie, M. R. J., 1963, The fundamentals of well log interpretations, 3rd ed.: Academic Press, New York, p. 238.
Wyllie, M. R. J., and Gregory, A. R., 1953, Formation factors of unconsolidated porous media: Influence of particle shape and effect of cementation: Trans. AIME, v. 198, p. 103–110.
Wyllie, M. R. J., and Rose, W., 1950, Some theoretical considerations related to the quantitative evaluation of physical characteristics of reservoir rock from electric log data: J. Petr. Tech., v. 2, p. 105–118.
Ziman, J. M., 1979, Models of disorder: New York, Cambridge University Press.

APPENDIX
THE EFFECT OF SHAPE ON EXPONENT

Equation (11) is easily generalized for a water-coated ellipsoid, following Stratton (1941),

$$\varepsilon^*_{xx} = \varepsilon^*_w \left[\frac{\varepsilon^*_w + (\varepsilon^*_m - \varepsilon^*_w)(1 - \phi + \phi L_x)}{\varepsilon^*_w + \phi L_x(\varepsilon^*_m - \varepsilon^*_w)} \right] \quad \text{(A–1)}$$

if one assumes that the anisotropy of the ε^* of the formation is not different from the grains. The shape of the coated grain is taken to be the same as that of the rock grain. In equation (A–1), L_x denotes the depolarizing factor associated with the principal x-axis along which the field is impressed. L_x depends upon the aspect ratio of the grain. For ellipsoids with axes a, b, c, the depolarization factor along a-axis is given by (see Stratton, 1941, for example)

$$L_a = \frac{1}{2} abc \int_0^\infty ds/(s + a^2)[(s + a^2)(s + b^2)(s + c^2)]^{1/2}. \quad \text{(A–2)}$$

For practical calculations, the following approximations are often useful (see Van Beek, 1967) for $a \gg b = c$ (prolate spheroid)

$$L_a \simeq [\ln(2a/b) - 1](b/a)^2; L_b = L_c = \frac{1}{2}(1 - L_a),$$

for $a \ll b = c$ (oblate spheroid)

$$L_a \to 1; L_b = L_c = \frac{1}{2}(1 - L_a),$$

and for spheres

$$L_a = L_b = L_c = 1/3.$$

Any electric field can be decomposed into three components parallel to the three axes of an arbitrarily oriented ellipsoid, and hence it is easy to consider arbitrary orientations of the ellipsoids. But for present purposes it is sufficient to consider a random array of ellipsoids of the same shape, arbitrary size, but fixed orientation with their principal axes parallel to each other. In other words, we take a fixed, scalar L for the entire assembly, and compute a specific component of the dielectric tensor. The effect of averaging over orientations has been considered by Mendelson and Cohen (1979). For spheres, setting $L = 1/3$ in equation (A–1) immediately gives back equation (11). From now on we drop the suffix x. For flat disks with their faces parallel to the impressed field or for needles with their axes parallel to the field, L is zero and equation (A–1) gives

$$\varepsilon^* = (1 - \phi)\varepsilon^*_m + \phi\varepsilon^*_w. \quad \text{(A–3)}$$

Equation (A–3) is identical to the exact result for dielectric constant of a medium made of layers of rock and water (with thicknesses smaller than the wavelength), for the case in which the

field is parallel to the interface. Similarly for disks with field impressed normal to the face $L = 1$, and equation (A–1) gives

$$1/\varepsilon^* = (1 - \phi)/\varepsilon_m^* + \phi/\varepsilon_w^*. \tag{A–4}$$

Equation (A–4) is identical to the exact dielectric constant of the layered medium with the field perpendicular to the interface.

Next, to show how the exponent m depends upon L, we rewrite equation (A–1) in the form of equation (12)

$$\frac{\varepsilon^* - \varepsilon_w^*}{L\varepsilon^* + (1 - L)\varepsilon_w^*} = (1 - \phi)\frac{\varepsilon_m^* - \varepsilon_w^*}{L\varepsilon_m^* + (1 - L)\varepsilon_w^*}. \tag{A–5}$$

A self-similar model can be generated, just as in the text. We find, following the steps outlined in the text, that the dielectric constant ε^* for the self-similar model is given by

$$\left(\frac{\varepsilon_m^* - \varepsilon^*}{\varepsilon_m^* - \varepsilon_w^*}\right)\left(\frac{\varepsilon_w^*}{\varepsilon^*}\right)^L = \phi. \tag{A–6}$$

For spheres $L = 1/3$ this gives equation (21).

Next consider the dc limit, for which equation (A–6) gives

$$\sigma = \sigma_w \phi^{1.1 - L}. \tag{A–7}$$

For spheres $L = 1/3$, this gives $\sigma = \sigma_w \phi^{3/2}$. For $L \to 1$, $\sigma \to 0$ (since $\phi < 1$); and for $L = 0$, needles with axes parallel to the field, $\sigma = \sigma_w \phi$. For cylinders with their axes perpendicular to the field $L = 1/2$, equation (A–6) gives

$$\sigma = \sigma_w \phi^2. \tag{A–8}$$

This is clearly an unrealistic model for the microgeometry of the rock, and it may be misleading to infer anything from this result. The correct procedure is clearly to average over different values of L (e.g., Mendelson and Cohen, 1979).

For samples containing platey materials, σ can be small. For example, for $L = 0.9$, $\sigma = \sigma_w \phi^{10}$. This is in qualitative agreement with observations of Jackson et al (1978). The plates effectively block the conducting path. We note for completeness the generalization of equation (15), for spheroidal rock grains (impurity) distributed in the water host, gives Fricke's (1924) formula

$$\sigma = \sigma_w \frac{y\phi}{y + 1 - \phi}, \tag{A–9}$$

where $y = (1 - L)/L$ 2 for spheres.

Returning now to equation (A–1), the boundary value problem solved to obtain it is modified when the anisotropy of the dielectric constant of the formation is included. Equations (A–1), (A–5), and (A–6) result with L redefined to include implicitly the anisotropy of ε^*, as has been shown by Mendelson and Cohen (1979), but our results remain quantitatively correct for the three cases $L = 0$ (needles), $L = 1/3$ (spheres), and $L = 1$ (plates).